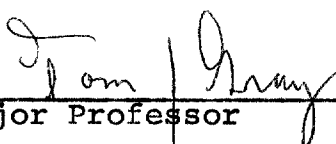
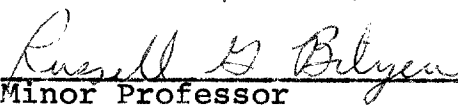
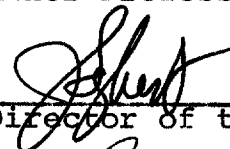


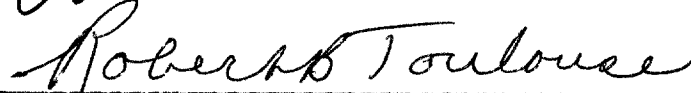
(N,2N) CROSS SECTION MEASUREMENTS IN
PRASEODYMIUM-141 AS A FUNCTION
OF NEUTRON BOMBARDING ENERGY

APPROVED:


Major Professor


Minor Professor


Director of the Department of Physics


Dean of the Graduate School

Marsh, Stephen Addison, (N,2N) Cross Section Measurements in Praseodymium-141 As a Function of Neutron Bombarding Energy. Master of Science, (May 1971), 52pp., 6 tables, 3 illustrations, bibliography, 26 titles.

Using the parallel disk method of activation analysis, the (n,2n) reaction cross section in ^{141}Pr was measured as a function of neutron energy in the range 15.4 to 18.4 MeV. The bombarding neutrons were produced from the $^3\text{T}(d,n)^4\text{He}$ reaction, where the deuterons were accelerated by the 3-MV Van de Graff generator of the North Texas Regional Physics Laboratory in Denton, Texas. The measurements were made relative to the well known cross section for the $^{63}\text{Cu}(n,2n)^{62}\text{Cu}$ reaction.

The requirement implicit in the flux monitor technique is that the neutron flux experienced by each sample is the same. This enables complicated calculations of the neutron flux to be eliminated. The induced activities were, therefore, measured and related by appropriate equations to the cross section. The activity of each sample was followed by a $1\frac{1}{2}$ by $1\frac{1}{2}$ inch NaI(Tl) detector in conjunction with a 400 channel analyser.

The neutron energies were determined by geometrical means. A frequency was assigned to each possible energy that intercepted the samples. These frequencies were then used to calculate the mean neutron energy striking the samples within one standard deviation.

The experimental cross section was determined from standard activation analysis equations. Because the cross section equation possesses several independent variables, each of which is subject to randomness, care was taken to account for any errors which might have occurred in their determination. This would include any errors inherent in the experimental procedure.

A condensed version of the statistical model of the compound nucleus is given in addition to a unique approach to the characteristics of the nuclear temperature. The results of the calculations using this nuclear temperature give a far more acceptable shape to the excitation curve. The results of the parallel disk data are in close agreement with the theoretical predictions and the results of two other laboratories.

(N,2N) CROSS SECTION MEASUREMENTS IN
PRASEODYMIUM-141 AS A FUNCTION
OF NEUTRON BOMBARDING ENERGY

THESIS

Presented to the Graduate Council of the
North Texas State University in Partial
Fulfillment of the Requirements

For the Degree of

MASTER OF SCIENCE

By

Stephen Addison Marsh, B. S.

Denton, Texas

May, 1971

TABLE OF CONTENTS

	Page
LIST OF TABLES	ii
LIST OF ILLUSTRATIONS	iii
Chapter	
I. INTRODUCTION	1
II. EXPERIMENTAL METHOD	5
III. DETERMINATION OF NEUTRON ENERGIES	9
IV. EXPERIMENTAL CROSS SECTION	16
V. STATISTICAL MODEL OF THE COMPOUND NUCLEUS	24
VI. RESULTS AND CONCLUSIONS	38
APPENDIX	44
REFERENCES	51

LIST OF TABLES

Table	Page
1.1	Q-values for Neutron Induced Reactions in ^{141}Pr . . . 4
6.1	$^{141}\text{Pr}(n,2n)^{140}\text{Pr}$ Cross Sections 39
6.2	$^{141}\text{Pr}(n,2n)^{140}\text{Pr}$ Cross Section by Parallel Disk Method 41
I.	$^{63}\text{Cu}(n,2n)^{62}\text{Cu}$ Cross Sections 44
II.	Parameters Used in the Equation for the Experimental Cross Section 45
III.	Cameron's Parameters Used in the Equations for the Theoretical Cross Section 46

LIST OF ILLUSTRATIONS

Figure		Page
2.1	Deuteron Energy vs. Hall Probe Voltage	7
3.1	Target-Sample Geometry	12
6.1	Praseodymium Cross Section vs. Neutron Energy . . .	42

CHAPTER I

INTRODUCTION

Detailed information concerning the nature of fast neutron reactions is frequently used in reactor studies dealing with threshold detectors. The accuracy of the excitation curve of the corresponding reactions is desired to be on the order of ± 5 percent. It will, therefore, be the purpose of this paper to examine the $^{141}\text{Pr}(n,2n)^{140}\text{Pr}$ reaction cross section as a function of neutron bombarding energy.

The importance in obtaining a consistent set of values for the $^{141}\text{Pr}(n,2n)^{140}\text{Pr}$ cross section is twofold: (i) the gamma spectrum of ^{140}Pr is extremely clean; and, (ii) ^{140}Pr has a short half-life. Thus, these measurements are needed to extend the range over which the $^{141}\text{Pr}(n,2n)^{140}\text{Pr}$ reaction may be used to provide a useful flux monitor for measuring cross sections of short half-life samples. Moreover, if an adequate representation of the cross section is to be obtained, it must be measured as a function of neutron bombarding energy.

Although several experiments ³⁻⁷ have reported the cross section for the $^{141}\text{Pr}(n,2n)^{140}\text{Pr}$ reaction near 14Mev, only a few have given results as a function of neutron bombarding energy. Ferguson and Thompson ⁸ first measured the $^{141}\text{Pr}(n,2n)^{140}\text{Pr}$ reaction cross section at neutron energies

9

ranging from 12.5 to 18 Mev. Bormann , et al. have also reported the cross section in the neutron energy range 12.6 to 19.6 Mev. The experimental results from both of these laboratories exhibit close agreement with the theoretical predictions set forth by the statistical model of the compound nucleus.

10

Weisskopf and Ewing have proposed a theoretical approximation for $(n,2n)$ cross sections as a function of neutron bombarding energy for nuclides with mass number greater than fifty. Their equation, however, possesses two parameters which are in general not known: The cross section for the emission of one neutron from the compound nucleus; and, the nuclear temperature. The cross section for the emission of at least one neutron from the compound nucleus would, ideally, be the sum of the cross sections for all the reactions which would involve the emission of one neutron. It is impossible, however, to know all of the cross sections, and especially as a function of neutron bombarding energy. On the other hand, this cross section can be approximated with the results being quite acceptable.

The $T(d,n) \text{ } ^3_2\text{He}$ reaction was utilized to produce neutrons to measure the $(n,2n)$ reaction cross section in praseodymium. The deuterons in the $T(d,n) \text{ } ^3_2\text{He}$ reaction were accelerated by the 2MV Van de Graff accelerator of the North Texas Regional Nuclear Physics Laboratory, which produced neutrons from the reaction in the energy range 15.4 to 18.4 Mev at 0° in the laboratory system.

An examination of the Q-values¹¹, Table 1.1, for neutron induced reactions in praseodymium indicate that several reactions are possible. However, at the neutron energies mentioned, the (n,2n) process is highly dominant and may be regarded as a measure of the total cross section. To determine the praseodymium cross section, the flux monitor technique of cross section analysis was employed; where, copper was used as a flux monitor. Copper was chosen because the ⁶²Cu isotope has a half-life² which is comparable to that of ¹⁴⁰Pr and the ⁶³Cu(n,2n)⁶²Cu cross section is well known.

TABLE 1.1

Q-VALUES FOR NEUTRON INDUCED REACTIONS IN ^{141}Pr

Reaction	Q-Value (KeV)
$^{141}\text{Pr}(n,\gamma)^{142}\text{Pr}$	5836
$^{141}\text{Pr}(n,p)^{141}\text{Ce}$	202
$^{141}\text{Pr}(n,d)^{140}\text{Ce}$	-3102
$^{141}\text{Pr}(n,t)^{139}\text{Ce}$	-5910
$^{141}\text{Pr}(n,^3\text{He})^{139}\text{La}$	-5620
$^{141}\text{Pr}(n,\alpha)^{138}\text{La}$	6180
$^{141}\text{Pr}(n,2n)^{140}\text{Pr}$	-9368
$^{141}\text{Pr}(n,np)^{140}\text{Ce}$	-5326
$^{141}\text{Pr}(n,2p)^{140}\text{La}$	-8317

CHAPTER II

EXPERIMENTAL METHOD

Fast neutrons for this experiment were produced by the $T(d,n) He$ reaction, where the deuterons were accelerated by the 2MV Van de Graff accelerator of the North Texas Regional Physics Laboratory. The tritium target, obtained from Texas Nuclear consisted of a 1-inch copper foil onto which had been evaporated a $1mg/cm^2$ layer of titanium which was later converted to titanium tritide, with the tritium content being approximately from three to five curies.

A bending magnet was used for momentum analysis and energy control of the beam. After being bent through an angle of 25° the deuteron beam passed through a slit assembly which monitored any fluctuations in beam spread. When the beam would fall on one slit more than the other, the potential difference produced would initiate a signal to be sent via a d.c. amplifier to the corona points. The corona load would then be either increased or decreased, thus maintaining a constant beam energy spread. The accelerating system was maintained at 10^{-6} mm of Hg throughout the experiment.

A Hall probe located at the center of the magnet measured the field strength of the magnet. When the magnet power supply current was changed, hence changing the field strength of the magnet, a potential difference would be produced in

the Hall probe. This Hall probe voltage was calibrated to deuteron bombarding energy by the well known (p,γ) and (p,n) resonance reactions on a lithium fluoride target. The deuteron beam energy was therefore known with a deviation of ± 5 KeV at the tritium target. Figure 2.1 shows the energy of deuterons as a function of the Hall probe voltage.

The experimental procedure adopted for irradiating samples and measuring the induced activities of the samples has been described in detail in earlier papers.^{12,13} The requirement implicit in the flux monitor technique is that the neutron flux experienced by each sample is the same. This enables complicated calculations of the neutron flux to be eliminated.

For the parallel disk method, copper disks were obtained from Alpha Inorganic with chemical purity of 99.99 per cent. Praseodymium disks were cut from a 5 mil foil to the same geometrical size as the copper disks. The chemical purity of the praseodymium was cited by Alpha Inorganic to be 99.99 per cent. The disks were 3/8 inch in diameter and 5 mil in thickness.

Praseodymium disks were stored in oil when not in use and were coated with grease during activation analysis, due to the high oxidizing properties of the metal. Samples of grease and oil were irradiated and displayed no activation.

For a typical activation analysis, the praseodymium and copper disks were placed in a nylon holder approximately 3/8 inch from the tritium target. Exposure time to neutron

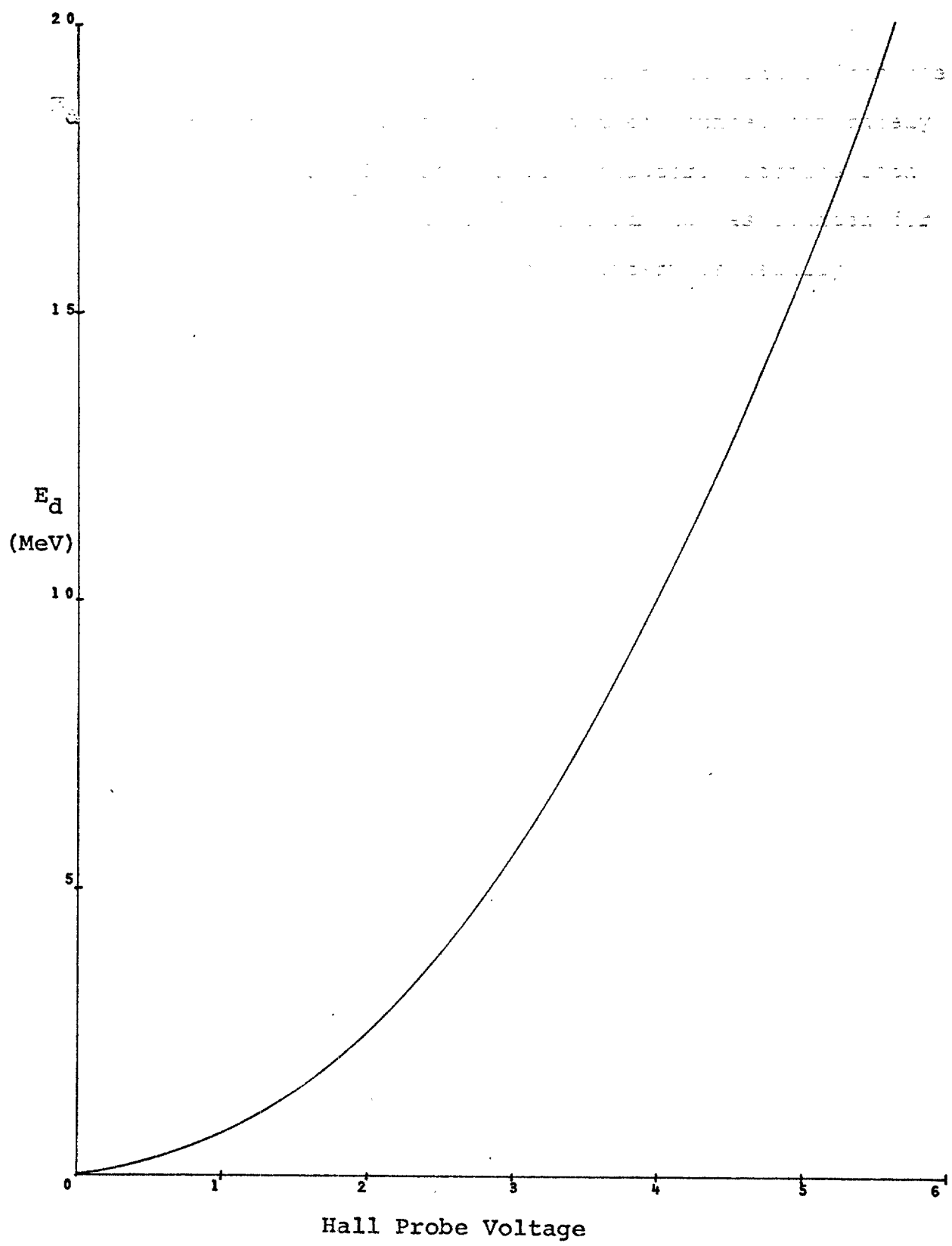


Figure 2.1

bombardment was six minutes for each run. The activated samples were prepared for counting within one minute from the end of activation. The samples were then counted separately with a 1 inch by 1 1/2 inch NaI(Tl) detector. Because both $^{140}_{62}\text{Pr}$ and $^{140}_{63}\text{Cu}$ are β emitters, each sample was counted for annihilation radiation with counting intervals usually lasting seven minutes.

CHAPTER III

DETERMINATION OF NEUTRON ENERGIES

The kinematics of the two-body nuclear reaction predict the Kinetic energy of the emitted neutron will be given in the laboratory coordinate system by

$$\sqrt{E_n} = \frac{(m_\alpha m_n E_d)^{1/2} \cos \theta}{m_\alpha + m_n} \pm \left(\frac{m_d m_n E_d \cos^2 \theta}{(m_\alpha + m_n)^2} + \frac{(m_\alpha - m_d) E_d + m_\alpha Q}{m_\alpha + m_n} \right)^{1/2} \quad (3.1)$$

where,

E_n = Kinetic energy of the neutron

E_d = Kinetic energy of the deuteron

m_d = Rest mass of the deuteron

m_n = Rest mass of the neutron

m_α = Rest mass of the alpha particle

θ = Angle between the incident deuteron and the emitted neutron

Q = Q value for the reaction

Equation (3.1) can be written as

$$\sqrt{E_n} = A \pm \sqrt{A^2 + B} \quad (3.2)$$

where

$$A = \frac{(m_d m_n E_d)^{1/2} \cos \theta}{m_\alpha + m_n} \quad \text{and} \quad B = \frac{(m_\alpha - m_d) E_d + m_\alpha Q}{m_\alpha + m_n} \quad (3.3)$$

Since the Q value for the ${}^3\text{T}(d,n){}^4\text{He}$ reaction is positive and since m_α is greater than m_d ,

$$\sqrt{A^2 + B} > A \quad (3.4)$$

Thus, for neutron energies of physical significance

$$\sqrt{E_n} = A + \sqrt{A^2 + B} \quad (3.5)$$

This equation when squared gives the energy of the emitted neutron as a function of deuteron bombarding energy and angular distribution in the laboratory system.

It is important to note that the positioning of the sample relative to the tritium target reflects directly upon the activity produced. Examination of equation (3.1) infers that at large separation distances of the sample from the target, only those neutrons of energy characterized by small θ will intercept the sample. In other words, the target will appear as being a point source. This situation is ideal for an approach to monoenergetic neutrons intercepting the sample; however, the resultant activity produced is small. On the otherhand, small separation distances will produce high activity, but the neutron energy spread experienced by the sample is quite large due to the large number of possible values for θ . If the separation distance is chosen such that a suitable amount of activity is produced in the sample and the neutron energy spread is small in comparison to E_n , the following derivation

is valuable for determining the mean neutron energy experienced by the sample.

The effective size of the tritium target will be assumed to be circular and characterized by the size of the deuteron beam spot. The target T (Figure 3.1) is considered to be a collection of point sources, each of which will emit a homogeneous neutron flux; that is, each value of θ is equally likely as another.

For a point source P located a distance h from the center of the target, neutrons of energy given by θ and E_d will describe a circle of radius $d \tan\theta$. This circle, when intersecting the sample S, will give the effective contribution of the solid angle defined by θ . The angle ϕ in the (x,y) plane locates the arbitrary area element dA given by

$$dA = r' d \tan\theta \cos\theta d\phi d\theta \quad (3.6)$$

where

$$r' = d(1 + \tan^2\theta)^{1/2} \quad (3.7)$$

is the distance from P to dA and d is the separation distance of the sample from the target. Because the solid angle θ encompasses every angle from 0 to θ , it is desirable to know the area A of the ring between θ and $\theta + d\theta$:

$$A = \int_{\theta}^{\theta + d\theta} \int_{-\phi_{\max}}^{\phi_{\max}} r' d \tan\theta \cos\theta d\phi d\theta \quad (3.8)$$

The maximum value for ϕ will be at the intersection of the

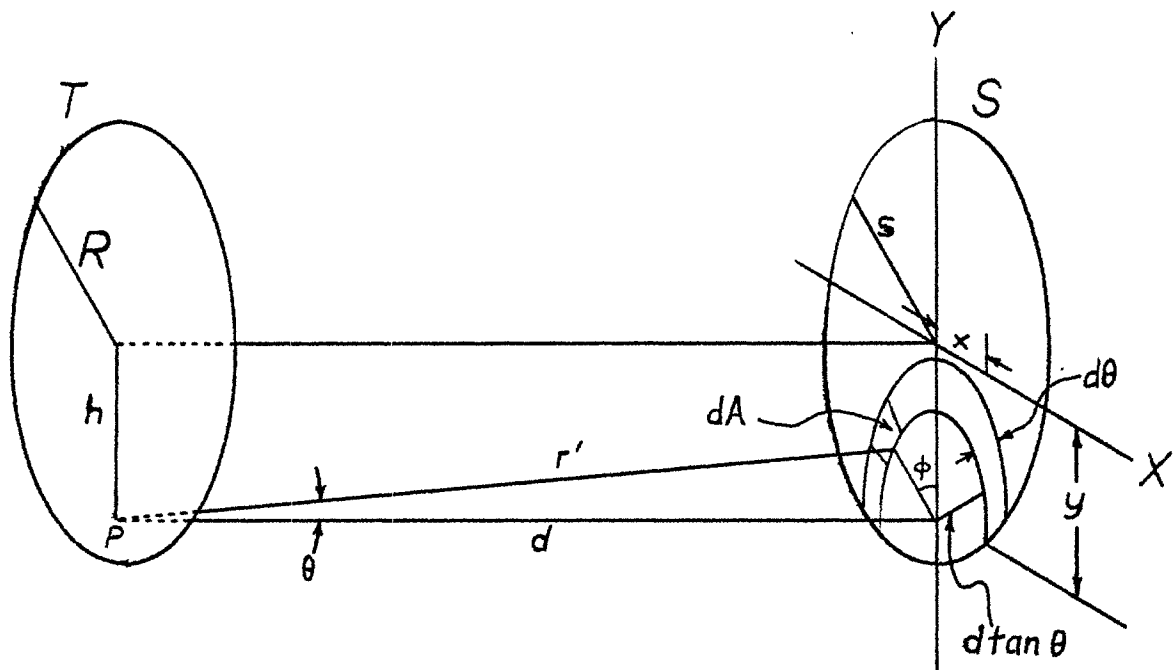


Figure 3.1
Target - Sample Geometry

circle

$$x^2 + y^2 = s^2 \quad (3.9)$$

and the circle

$$x^2 + (y-h)^2 = d^2 \tan^2 \theta \quad (3.10)$$

or

$$\phi_{\max} = \arctan\left(\frac{x}{y-h}\right) \quad (3.11)$$

where y and x are determined from equations (3.9) and (3.10)

to be

$$y = \frac{s^2 + h^2 - d^2 \tan^2 \theta}{2h} \quad (3.12)$$

and

$$x = \sqrt{d^2 \tan^2 \theta - (y-h)^2} \quad (3.13)$$

Thus, equation (3.8) becomes for a particular h

$$A = \int_{\theta}^{\theta+d\theta} 2d^2 (1+\tan^2 \theta)^{1/2} \tan \theta \cos \theta \times \arctan \left[\frac{\sqrt{d^2 \tan^2 \theta - [(s^2 - h^2 - d^2 \tan^2 \theta)/2h]^2}}{(s^2 - h^2 - d^2 \tan^2 \theta)/2h} \right] d\theta \quad (3.14)$$

The maximum value of θ will be the largest possible solid angle intersecting S ; or,

$$\theta_{\max} = \arctan$$

Further conditions on equation (3.14) are

$$\phi_{\max} = \begin{cases} 2\pi, h+d\tan\theta < s \\ 0, s+d\tan\theta < h \end{cases} \quad (3.16)$$

Because ϕ is a function of θ and h , equation (3.13) can be calculated numerically. The effective contribution of any θ_i can be summed over all possible values of h_j ; or

$$A_{ij} = \sum_j f(\theta_i) \phi(\theta_i, h_j) \quad (3.17)$$

where the quantity A_{ij} represents the area of the ring intercepted by S for a particular θ_i and h_j . If the sum over j is first executed, the area A_{ih} represents the frequency by which neutrons of energy E_i will intercept the sample S . Thus, the mean energy E_{mean} for all possible values of E_i is

$$E_{\text{mean}} = \frac{\sum_i (A_{ih} E_i)}{\sum_i A_{ih}} \quad (3.18)$$

Hence, the standard deviation may be written as

$$\text{S.D.} = \sqrt{\frac{\sum_i (A_{ih} E_i^2) - (\sum_i A_{ih} E_i)^2}{\sum_i A_{ih}}} \quad (3.19)$$

The assumptions upon which the preceding derivations are based do not account for any variations which are inherent in the ${}^3\text{T}(d,n){}^4\text{He}$ reaction. In actuality, the incident deuteron energy will have a spread of ± 1 per cent due to fluctuations in the accelerating voltage and marginal error in the Hall probe calibration. Other variations such as self shadowing of the sample, finite size of the beam spot, deuteron

energy loss in the tritium target, distribution of the tritium in the target are analysed in detail in a previous paper.¹³ A combination of all the variations contributes ± 1 per cent to the neutron energy.

With these considerations, equations (3.13), (3.17), and (3.18) were calculated by virtue of the computer program MARSHEN which is reproduced in Appendix B.

CHAPTER IV

EXPERIMENTAL CROSS SECTION

Due to the great difficulty in obtaining direct measurements from neutron induced reactions, the cross section must be inferred from the radioactive nuclei produced from the reaction. It is, therefore, imperative to develop an expression for the cross section which is dependent upon the experimental capabilities mentioned heretofore. The following derivation is well known in reaction analysis for constructing the experimental cross section.¹²

The rate of formation of a radioisotope under an irradiation is directly proportional to the number of target nuclei, the incident neutron flux, and the cross section of the target nuclei. If N_0 target nuclei of cross section σ are subjected to a neutron flux ϕ , the rate of formation of N_a product nuclei is given by

$$\frac{dN_a}{dt} = \sigma \phi N_0 \quad (4.1)$$

Since at the beginning of the irradiation there are no, or few, radioactive nuclei present, the rate of decay of the product nuclei is insignificant to the rate of formation and the activity will grow linearly with time. However, as the population of radioactive nuclei increases, the decay rate becomes greater

and the net production decreases. As always, this rate of decay is proportional to the number of radioactive nuclei present

$$\frac{dN_a}{dt} = -\lambda N_a \quad (4.2)$$

where, λ is the decay constant. Thus, the final net production rate is given by the rate of formation of the product nuclei plus the rate of decay of the product nuclei

$$\frac{dN_a}{dt} = \sigma\phi N_0 - \lambda N_a \quad (4.3)$$

Separation of variables and direct integration gives

$$-\frac{1}{\lambda} \ln(\sigma\phi N_0 - \lambda N_a) = t + c \quad (4.4)$$

From the initial conditions at $t=0$, $N_a=0$, the integration constant C is determined to be

$$C = -\frac{1}{\lambda} \ln(\sigma\phi N_0) \quad (4.5)$$

Thus, equation (4.4) can be written as

$$N_a = \frac{\sigma\phi N_0}{\lambda} (1 - e^{-\lambda t_i}) \quad (4.6)$$

where t_i represents the total exposure time to the irradiation.

The total number of transitions during the counting interval can now be related to the total number of active

nuclei produced at the end of the irradiation. If t_1 represents the time lapse from the end of activation to the start of the counting, the number of active nuclei present is given by

$$N_1 = N_a e^{-\lambda t_1} \quad (4.7)$$

If t_2 represents the time lapse from the end of activation to the end of the counting, the number of active nuclei present is given by

$$N_2 = N_a e^{-\lambda t_2} \quad (4.8)$$

Thus the total number of transitions during the counting interval t_1 to t_2 , is

$$N = N_a (e^{-\lambda t_1} - e^{-\lambda t_2}) \quad (4.9)$$

Substitution of equation (4.6) into equation (4.9) yields

$$N = \frac{\sigma \phi N_0}{\lambda} (1 - e^{-\lambda t_i}) (e^{-\lambda t_1} - e^{-\lambda t_2}) \quad (4.10)$$

For multiple decay of an excited nucleus to any particular level of the residual nucleus, the number of transitions observed, N_B , is related to the total number of transitions, N , by the branching ratio B to that particular level. The relation may be written as

$$N_B = BN \quad (4.11)$$

Suppose that the excited nucleus decays in this manner to a level of the residual nucleus which in turn decays by gamma emission to another level. For nuclei of large mass number and dense electron clouds, there is a definite probability that the gamma will impart its energy to an electron; thus, not being detected. If N_e represents the number of internally converted electrons and N_γ the number of gammas, then

$$N_B = N_e + N_\gamma \quad (4.12)$$

The internal conversion coefficient is defined as

$$\alpha \equiv N_e / N_\gamma \quad (4.13)$$

then

$$N_B = (1 + \alpha) N_\gamma \quad (4.14)$$

Of the gamma transitions N_γ only a fraction G will be intercepted by the detector (due to geometry factors between the source and the detector); moreover, only a fraction f will undergo photoelectric interaction with the crystal. Thus, the total number of counts N_p under a photopeak is given by

$$N_p = fGN_\gamma \quad (4.15)$$

Thus, equation (4.10) is given by

$$N_p = \frac{BfG\sigma\phi N_0}{\lambda(1+\alpha)} (1 - e^{-\lambda t_1}) (e^{-\lambda t_1} - e^{-\lambda t_2}) \quad (4.16)$$

Expressing this equation in terms of the cross section results in

$$\sigma = \frac{\lambda(1+\alpha)N_p}{BfG N_0(1-e^{-\lambda t_1})(e^{-\lambda t_1}-e^{-\lambda t_2})} \quad (4.17)$$

Since the decay constant is given by

$$\lambda = .693/T \quad (4.18)$$

where T equals half-life, and the original number of target nuclei is given by

$$N_0 = \frac{N_A}{A} mP \quad (4.19)$$

where,

N_A = Avogadro's number

m = mass of sample

A = atomic number of the isotope

P = percentage abundance of the isotope

the cross section may be written as

$$\sigma = \frac{(1+\alpha)N_p A}{TBf\phi m P N_A(1-e^{-\lambda t_1})(e^{-\lambda t_1}-e^{-\lambda t_2})} \quad (4.20)$$

Based on the assumption that the flux experienced by the praseodymium disk is the same as that for the copper monitor, the cross section for the praseodymium may be expressed in terms of the cross section for copper:

$$\sigma(\text{Pr}) = \frac{1+\alpha(\text{Pr})}{1+\alpha(\text{Cu})} \frac{N_p(\text{Pr})}{N_p(\text{Cu})} \frac{141T(\text{Cu})B(\text{Cu})f(\text{Cu})G(\text{Cu})m(\text{Cu})P(\text{Cu})}{63T(\text{Pr})B(\text{Pr})f(\text{Pr})G(\text{Pr})m(\text{Pr})P(\text{Pr})}$$

$$\sigma(\text{Cu}) \times \frac{1-e^{-\lambda(\text{Cu})t_1}}{1-e^{-\lambda(\text{Pr})t_1}} \frac{e^{-\lambda(\text{Cu})t_1(\text{Cu})}-e^{-\lambda(\text{Cu})t_2(\text{Cu})}}{e^{-\lambda(\text{Pr})t_1(\text{Pr})}-e^{-\lambda(\text{Pr})t_2(\text{Pr})}} \quad (4.21)$$

The cross section for praseodymium is seen to be a function of several independent variables, each of which is subject to randomness. The cross section may be written as

$$\sigma = \sigma(x_1, x_2, x_3, \dots, x_n) \quad (4.22)$$

where the independent variable $x_1, x_2, x_3, \dots, x_n$ correspond to the quantities $N_p(\text{Pr}), N_p(\text{Cu}), \dots, \sigma(\text{Cu})$ in equation (4.21). For small variations in $x_1, x_2, x_3, \dots, x_n$ from their mean values, denoted by $\Delta x_1, \Delta x_2, \dots, \Delta x_n$, the resulting variation of σ from its mean can be written as ¹⁴

$$\Delta\sigma = \frac{\partial\sigma}{\partial x_1} \Delta x_1 + \frac{\partial\sigma}{\partial x_2} \Delta x_2 + \dots + \frac{\partial\sigma}{\partial x_n} \Delta x_n \quad (4.23)$$

ignoring differentials of higher order. Squaring equation (4.23) results in

$$(\Delta\sigma)^2 = \left(\frac{\partial\sigma}{\partial x_1}\right)^2 (\Delta x_1)^2 + \dots + \left(\frac{\partial\sigma}{\partial x_n}\right)^2 (\Delta x_n)^2 \quad (4.24)$$

where cross terms have been neglected. The standard deviation of σ may be taken as being the square root of the mean-square variance given by equation (4.24):

$$\text{S.D.} = \left[\left(\frac{\partial \sigma}{\partial x_1} \right)^2 (\Delta x_1)^2 + \dots + \left(\frac{\partial \sigma}{\partial x_n} \right)^2 (\Delta x_n)^2 \right]^{1/2} \quad (4.25)$$

The standard deviation for equation (4.21) can, hence, be written as

$$\text{S.D.} [\sigma(\text{Pr})] = \sigma(\text{Pr}) \left[\left(\frac{\Delta N_p(\text{Pr})}{N_p(\text{Pr})} \right)^2 + \dots + \left(\frac{\Delta \sigma(\text{Cu})}{\sigma(\text{Cu})} \right)^2 \right]^{1/2} \quad (4.26)$$

The important qualifications of equation (4.26) are that each variable be independent of the other. The variance of any particular variable from its mean is given by the probable error in its determination. If this variance is not known, it will be taken to be the square root of the mean value.

As mentioned previously, the activities of the praseodymium and copper produced from irradiation were measured by counting the annihilation radiation of each. Because the annihilation gammas originate outside the atom, there are no internally converted electrons; consequently, the internal conversion coefficient is taken to be zero for both copper and praseodymium. It is also found that the ratio of the efficiency factors $f(\text{Cu})/f(\text{Pr})$ is unity. This is due to the fact that the energy of the gammas counted is the same for each sample.

The quantities N_p, m, t_i, t_1 , and t_2 were determined from the experiment. All other quantities were accepted from the literature. Several values for the $^{63}\text{Cu}(n,2n)^{62}\text{Cu}$ reaction

cross section have been reported and are summarized in Table I of Appendix A. The other parameters in equations (4.21) and (4.25) and is reproduced in Table II of Appendix A.

CHAPTER V

STATISTICAL MODEL OF THE COMPOUND NUCLEUS

The statistical theory gives an account of $(n,2n)$ reactions with mass number greater than fifty, in terms of a rather simple model. If the variation of cross section with energy for this type of reaction is known, deductions about the effective energy level densities in the nuclei concerned can be made. The following theory¹⁵ is oriented toward the basic purpose of the paper; that is, to investigate the $(n,2n)$ cross section of praseodymium as a function of neutron bombarding energy and even more in particular to relate the resultant data to the statistical model of the compound nucleus.

In 1936, Niels Bohr¹⁶ made the assumption that a nuclear reaction may be divided into two stages: (i) the formation of an intermediate semi-stable system composed of the original nucleus X and the incident particle a; and, (ii) the subsequent decay of this compound system C into the products of the reaction, Y and b.



When the compound system C is formed there is a time in which the incident particle spends in complicated motion in the nucleus sharing its energy with all constituents. Finally, there is enough energy distributed to one or more

elementary or complex particles such that the compound system breaks up into a residual nucleus Y and outgoing particle b. Thus, the mode of decay of the compound system is regarded as being completely independent from the first stage of the collision process.

The Bohr assumption is based on a nucleus of strong interactions and short range forces. When the incident particle comes within the range of the nuclear force, its energy will be shared quickly with the other nucleons of the target nucleus. In other words, the mean free path Λ of a nucleon entering nuclear matter is very much smaller than the nuclear radius. This is true if the incident energy is not too high. An approximation of the mean free path Λ is given by¹⁵

$$\Lambda \approx 1.8 \times 10^{-15} (E + E_0) \text{ cm} \quad (5.2)$$

where E is the energy of the incident particle and E_0 is the average kinetic energy of the nucleons within the nucleus.

The compound nucleus acquires an excitation energy $E' = E + S_a$ where, S_a is the separation energy of the particle a from the compound nucleus. A large variety of nuclear reactions is possible here, depending upon those particles which require less than this excitation energy for emission from the compound nucleus. Clearly, if the excitation energy per nucleon is very much smaller than the average separation energy S of a particle from the compound system, it will take

a great many energy exchanges, and, hence, a long time before enough energy is distributed to one particle for its emission from the compound system.

Thus, the criteria for the validity of the Bohr assumption are that the mean free path λ of the entering nucleon be very much smaller than the nuclear radius R , and the average separation energy of a nucleon, or

$$\lambda \ll R \qquad E \ll (A-1)S \qquad (5.3)$$

These conditions necessitate the independence of the two stages (i) and (ii) of the collision process. Upon entering the nucleus, the incident particle quickly shares its energy with all constituents and thus has lost all identity as to its origin. The thorough mixing of the energy of the nucleons implies that the mode of decay of the compound system depends only on its energy, angular momentum, and parity, but not on the specific manner in which it was formed.

Although the above conditions are necessary but not sufficient, they will be regarded as correct in so far as this paper is concerned. The conditions are found to be fulfilled for nuclei with $A > 50$ and incident energies $E < 30 \text{ MeV}$; which are well within the realm of this paper.

The cross section for a nuclear reaction $X(a,b)Y$ can be inferred directly from the Bohr assumption:

$$\sigma(a,b) = \sigma_c(a)G_c(b) \qquad (5.4)$$

where, $\sigma_C(a)$ is the cross section for the formation of the compound system by a particle a incident upon the nucleus X . $G_C(b)$ is the probability that the compound system C , once formed, will decay by the emission of the particle b .¹⁵

An approximate description of $\sigma_C(a)$ can be obtained if the following assumptions regarding the structure of the nucleus are made:¹⁵

- (i) The nucleus has a well defined surface which is a sphere of radius R . The nuclear forces do not act between a and the center of the nucleus if the distance between a and the center of the nucleus is larger than R .
- (ii) If the particle a penetrates the nuclear surface, it moves with an average kinetic energy T_{in} , which is much higher than its energy E_a outside.
- (iii) Particle a is subject to very strong interactions inside the nucleus, so that it interchanges its energy rapidly with the other nucleons.
- (iv) The number of open channels is very large.

Classically, the assumption is that all particles hitting the surface of the nucleus will form a compound system. Under this consideration, the cross section $\sigma_C(a)$ can be given by the classical target area

$$\sigma_C(a) = \pi R^2 \quad (5.5)$$

A wave mechanical description alters the classical expression by allowing for the position of the particle a to be undefined within a wavelength λ . Also, due to the sudden change in potential when the particle crosses the nuclear surface, there is a possibility of reflection. If

$\psi(r)$ is the wave function corresponding to the relative motion of the particle a and the nucleus X , it can be written as a sum of partial waves of given angular momentum ℓ :

$$\psi(r) = \psi(r, \theta) = \sum_{\ell} \frac{u_{\ell}(r)}{r} Y_{\ell, 0}(\theta) \quad (5.6)$$

where, $u_{\ell}(r)$ is the radial wave function and $Y_{\ell, 0}(\theta)$ are the spherical harmonics.

The cross section $\sigma_c(a)$ can be subdivided into partial cross sections:

$$\sigma_c(a) = \sum_{\ell} \sigma_{c, \ell}(a) \quad (5.7)$$

where, $\sigma_{c, \ell}(a)$ is the cross section for the formation of the compound nucleus initiated by the particles with an angular momentum ℓ . It is, also, approximately correct to assume that particles with angular momentum ℓ move in the ℓ th zone with an uncertainty in position of λ . If T_{ℓ} , the transmission coefficient of the ℓ th partial wave, is the probability that a compound nucleus will be formed by particles of angular momentum ℓ , the cross section $\sigma_c(a)$ may be written as:

$$\sigma_c(a) = \pi \lambda^2 \sum_{\ell} (2\ell+1) T_{\ell} \quad (5.8)$$

It is more convenient to write equation (5.8) as:

$$\sigma_{c, \ell}(a) = \pi \lambda^2 (2\ell+1) (1 - |\eta_{\ell}|^2) \quad (5.9)$$

where, η_ℓ is the fraction of particles reflected or the relative amplitude of the outgoing wave with angular momentum ℓ .

The radial wave function $u_\ell(r)$ can be separated into incoming and outgoing waves:

$$u_\ell(r) = Au_\ell^{(-)}(r) + Bu_\ell^{(+)}(r) \quad (5.10)$$

where, A and B are constants. But, since η_ℓ is the fraction of particles reflected

$$u_\ell(r) = A \left[u_\ell^{(-)}(r) - \eta_\ell u_\ell^{(+)}(r) \right] \quad (5.11)$$

The logarithmic derivative f_ℓ , evaluated at the nuclear surface, is defined as

$$f_\ell \equiv R \left(\frac{1}{u_\ell(r)} \frac{du_\ell(r)}{dr} \right)_{r=R}$$

The logarithmic derivative is utilized in order to gain information about the wave functions describing the nucleon-nucleus interaction. The wave functions are solutions to the wave equation into which is inserted the nuclear potential. Thus, the logarithmic derivative depends upon the nuclear potential which describes the interaction.

$$e^{2i\xi} = u_\ell^{(-)}(R) / u_\ell^{(+)}(R) \quad (5.13)$$

and the penetration factor¹⁷ Δ_ℓ and the shift factor s_ℓ are defined as

$$R \left(\frac{1}{u_{\ell}^{(+)}(r)} \frac{du_{\ell}^{(+)}(r)}{dr} \right)_{r=R} = \Delta_{\ell} + i s_{\ell} \quad (5.14)$$

an equation for η_{ℓ} may be derived as

$$\eta_{\ell} = \frac{f_{\ell} - s_{\ell} + i \Delta_{\ell}}{f_{\ell} - s_{\ell} - i \Delta_{\ell}} \quad (5.15)$$

From these definitions the cross section $\sigma_{c,\ell}(a)$ is found to be

$$\sigma_{c,\ell}(a) = (2\ell+1)\pi\lambda^2 \frac{-4s_{\ell}\text{Im}(f_{\ell})}{[\text{Re}(f_{\ell}) - \Delta_{\ell}]^2 + [\text{Im}(f_{\ell}) - s_{\ell}]^2} \quad (5.16)$$

where,

$\text{Im}(f_{\ell})$ = imaginary part of the logarithmic derivative

$\text{Re}(f_{\ell})$ = real part of the logarithmic derivative

$$\Delta_{\ell} = R \left[\frac{G_{\ell} (dG_{\ell}/dr) + F_{\ell} (dF_{\ell}/dr)}{F_{\ell}^2 + G_{\ell}^2} \right]_{r=R}$$

$$s_{\ell} = R \left[\frac{G_{\ell} (dG_{\ell}/dr) - F_{\ell} (dF_{\ell}/dr)}{F_{\ell}^2 + G_{\ell}^2} \right]_{r=R}$$

$$F_{\ell}(r) = \left(\frac{\pi Kr}{2} \right)^{1/2} J_{\ell+1/2}(Kr) \quad (\text{for neutrons})$$

$$G_{\ell}(r) = \left(\frac{\pi Kr}{2} \right)^{1/2} N_{\ell+1/2}(Kr) \quad (\text{for neutrons})$$

$J_p(z)$ = spherical Bessel function of order p

$N_p(z)$ = spherical Neumann function of order p

k = $(2ME)^{1/2}/h$

M = reduced mass of a and x

E = incident energy of a

Since the penetration factor Δ_ℓ and the shift factor s_ℓ only relate information dealing with extranuclear interactions, the logarithmic derivative is the only quantity which specifies information to the cross section $\sigma_{c,\ell}(a)$ about intranuclear interactions. The logarithmic derivative can thus be specified by a nuclear model. One such model is the continuum model or strong interaction model or black nucleus model. Under the conditions set forth previously for the structure of the nucleus, assumption (iv) is particularly peculiar to the continuum model. This condition is met if the incident energy E is much higher than the first few excitation energies of the target nucleus.

Under these conditions the incident particle a , once it has penetrated the nuclear surface, is very unlikely to reappear in the entrance channel. It may well be reflected; however, if it penetrates the nucleus, by assumption (iv), it is very unlikely that the particle will leave by the entrance channel if many other channels are available.

In the continuum model, the entering particle moves within the nucleus with a high kinetic energy and immediately forms a compound nucleus sharing its energy with all other nucleons. Since the incident particle is assumed to form a compound nucleus and does not return, the wave function can be assumed to be that of an ingoing wave; that is,

$$u_{\ell}(r) \sim e^{-iKr} \quad r < R \quad (5.17)$$

where, K is the wave number of the interior region.

$$K = \frac{[2M(E+V_0)]^{1/2}}{\hbar} \quad (5.18)$$

Because the logarithmic derivative is continuous at the surface, the fundamental assumption of the continuum theory of nuclear reactions is

$$f_{\ell} = R \left(\frac{1}{u_{\ell}(r)} \frac{du_{\ell}(r)}{dr} \right)_{r=R} = -iKR \quad (5.19)$$

Thus, the equation (5.16) for cross section $\sigma_{c,\ell}$ for the continuum model results in

$$\sigma_{c,\ell}(a) = (2\ell+1)\pi\lambda^2 \frac{4s_{\ell}KR}{\Delta_{\ell}^2 + (KR+s_{\ell})^2} \quad (5.20)$$

such that

$$\sigma_c(a) = \pi\lambda^2 \sum_{\ell} (2\ell+1) \frac{4s_{\ell}KR}{\Delta_{\ell}^2 + (KR+s_{\ell})^2} \quad (5.21)$$

This equation for the cross section for the formation of the compound nucleus will be elaborated upon later in the chapter to show its significance and limitation.

Attention is now focussed to the decay of the compound nucleus. $G_c(b)$ is the dimensionless probability that the compound nucleus, once formed, will decay by the emission

of the particle b to the probability for the emission of all other particles:

$$G_c(b) = F_b / \sum_d F_d \quad (5.22)$$

where, F_d is the probability for the emission of particle d. The probability that the system will decay by one specific channel, $G_c(\beta)$, where β denotes this channel, is the ratio of the energy widths

$$G_c(\beta) = \Gamma_\beta / \sum_i \Gamma_i \quad (5.23)$$

where Γ_β is the partial width for emission of particle b into the specific channel β , and i denotes any possible exit channel.¹⁷ Weisskopf¹⁸ has shown that equation (5.23) may be written as

$$G_c(\beta) = \frac{\Gamma_\beta}{\sum_i \Gamma_i} = \frac{k_\beta^2 \sigma_c(\beta)}{\sum_i k_i^2 \sigma_c(i)} \quad (5.24)$$

where $k=1/\lambda$.

This "branching ratio", as it is sometimes named, is found to be dependent upon the level density of the residual nucleus and the maximum energy available for the emission of particle b. Moore¹⁷ determines an integral equation for $G_c(b)$ to be

$$G_c(b) = \frac{\int_0^{E'_b} k_b^2 \sigma_c(b) \rho_Y(E'_b - E_b) dE_b}{\sum_{\alpha} \int_0^{E'_\alpha} k_\alpha^2 \sigma_c(\alpha) \rho_Y(E'_\alpha - E_\alpha) dE_\alpha} \quad (5.25)$$

where E'_b denotes the maximum energy with which particle b may be emitted, and ρ_Y denotes the nuclear level density of the residual nucleus Y at excitation $E'_\alpha - E_\alpha$. For a nuclear reaction, the maximum energy E'_b of the emitted particle b is $E_a + Q_{ab}$, where E_a is the incident particle energy, and Q_{ab} is the Q value for the (a,b) reaction.

If the residual nucleus is considered as being a collection of nucleons, each of which is independent of the other, it can be assumed that each of them has a set of equally spaced single-particle energy levels. As the excitation energy increases, the single-particle level spacings decrease due to the greater number of ways of dividing the energy among the particles. The nuclear level density ρ_Y , therefore, rises rapidly with increasing excitation energy and atomic number. Because the levels will now possibly overlap, they cannot be treated individually and a statistical weight is assigned to the single-particle levels which will be a measure of the level density in the same energy region.

The approach for determining the level density is a statistical one and is expected to only give results that greatly oversimplify the actual situation with the orders of magnitude to be expected. The nucleus is likened to a

liquid drop. The excitation energy E is considered as heat which raises the nuclear temperature and consequently a particle is boiled off. From the Bohr assumptions, the process of evaporation of the particle is independent from the mode of formation of the compound nucleus, and depends only on its energy. The nuclear entropy $S(E)$ is introduced as

$$S(E) = \ln \rho(E) \quad (5.26)$$

When the particle is emitted from the compound nucleus, it will leave the residual nucleus at a temperature T defined as

$$T = \left[\frac{\partial S(E)}{\partial E} \right]^{-1} \quad (5.27)$$

The energy distribution of the evaporated particles is described by the classical Maxwellian distribution determined by the nuclear temperature T . The assumption can be made, therefore, that

$$E = aT^2 \quad (5.28)$$

The level density is therefore found to be

$$\rho(E) = C e^{2(aE)^{1/2}} = C e^{2E/T} \quad (5.29)$$

where C and a are constants.

For neutron induced reactions, the above analogy can be extended to derive the cross sections $\sigma(n, 2n)$, $\sigma(n, p)$, $\sigma(n, \alpha)$.

By appropriately modifying equations (5.25) and (5.29) the results may be written as¹⁸

$$\sigma(n,2n) = \sigma_C(n) \left[1 - \left(1 + \frac{E_C}{T} \right) e^{-E_C/T} \right] \quad (5.30)$$

and

$$\sigma(n,p) = \sigma_C(n) e^{E_p^*/T} \quad (5.31)$$

and

$$\sigma(n,\alpha) = 2\sigma_C(n) e^{E_\alpha^*/T} \quad (5.32)$$

where

$\sigma_C(n)$ = cross section for the formation of the compound nucleus induced by neutrons

T = temperature of the residual nucleus

E_C = $E_n + Q_{n,2n}$

E_n = energy of the incident neutron

$Q_{n,2n}$ = Q value for the $(n,2n)$ reaction

E_p^* = $Q_{n,p} + \delta_R - \delta_T - K_p V_p$

E_α^* = $Q_{n,\alpha} + \delta_R - \delta_T - K_\alpha V_\alpha$

δ_R = pairing energy for the residual nucleus

δ_T = pairing energy for the target nucleus

KV = Coulomb interaction term

Of particular interest here is the $(n,2n)$ cross section of praseodymium. The text by Blatt and Weisskopf¹⁵ recommend that for incident energies on the order of 15MeV that in the

case for praseodymium, the nuclear temperature is

$$T \sim 1.1 \text{ to } 1.5 \text{ MeV} \quad (5.33)$$

A more elaborate representation of the nuclear temperature is given by Cameron¹⁹

$$T = \frac{3}{\pi^2 G} \left[\frac{3}{2} + \left(\frac{9}{4} + \frac{2\pi^2 GU}{3} \right)^{1/2} \right] \quad (5.34)$$

where

U = excitation energy of the target nucleus

$G = G_Z + G_N$

G_Z = density of proton orbits at the Fermi level

G_N = density of neutron orbits at the Fermi level

Cameron uses the following equation to approximate G_Z and G_N :

$$G_k(T) = \frac{a_0(k) + a_1(k)T + a_2(k)T^2 + a_3(k)T^3 + a_4(k)T^4}{1 + T + T^2 + T^3 + T^4} \quad (5.35)$$

where k refers to Z or N and the constants $a_0(k) \dots a_4(k)$ are given in Cameron's paper. The values used for equations (5.30), (5.34), and (5.35) are cited in Table III of Appendix A. The determination of $\sigma_c(a)$ can be accomplished by numerical methods. The computer program COMPNUC²¹ was written to calculate $\sigma(n, 2n)$ for nuclei with mass number greater than fifty, using Cameron's nuclear temperature.

CHAPTER VI

RESULTS AND CONCLUSIONS

The cross section for the $^{141}\text{Pr}(n,2n)^{140}\text{Pr}$ reaction as measured by previous works is summarized in Table 6.1. Of particular interest here are the measurements of Ferguson and Thompson⁸, and Bormann⁹, et al. The method by which the excitation curve for these works is found is rather well known and widely used. As is usually the case for this method, 1MeV and 3MeV deuterons are used to establish separate sections of the excitation function. The angular variation of neutron flux is calculated from the differential relative cross section calculations from papers such as Bame and Perry²², and Paulsen and Liskien.²³ The two sets of data are then normalized to each other in the overlapping energy region, usually near 16.2 to 16.8MeV neutron energy. This relative excitation function is then normalized again to a well known absolute cross section measurement in the 14.0 to 14.5MeV region. This method is reported to have reproducibility on the order of ± 7 per cent.²⁴

The calculations of the neutron energies, cross section, and corresponding errors were executed by the computer program MARSHEN and the appropriate equations mentioned heretofore. The results are given in Table 6.2.

TABLE 6.1

 $^{141}\text{Pr}(n,2n)^{140}\text{Pr}$ Cross Section

Neutron Energy (MeV)	Cross Section (mb)	Reference
14.4	1801±135	3
14.5	2060±700	4
14.0	2002±225	5
14.8	1378±206	6
14.8	2100±300	7
12.41±.12	1231±111	8
13.77±.20	1386±125	
14.74±.27	1591±143	
15.78±.32	1737±156	
16.96±.34	1606±145	
17.98±.24	1667±150	
12.78±.11	1496±144	9
13.44±.13	1485±143	
14.11±.15	1614±159	
14.87±.17	1700±164	
15.52±.17	1787±172	
16.18±.18	1801±174	
16.85±.18	1872±180	
17.78±.17	1905±183	
18.56±.15	1853±178	
19.42±.12	1804±174	

Error analysis for cross section calculations included any variations in irradiation timing, counting intervals, mass determinations, geometry, efficiency, and literature values. Compounded quadratically, the error in cross section determination is of the order of ± 8 per cent. The largest contribution to the error stems from the quoted errors in the $(n,2n)$ cross section for the copper monitor. If only the experimental variations of this work are considered, the excitation curve would be accurate to about ± 6.6 per cent. Evidence of this fact is the measurement at 17MeV where the reproducibility is seen to be quite strong.

The results of this work and the results of previous publications are displayed in Figure 6.1 with the solid curve representing the results from COMPNUC²¹ for the compound nucleus theory. The data tend to be in close agreement with Ferguson and Thompson, and Bormann, et al. As a whole, the experimental excitation function contends to be lower than theory predicts, especially at energies greater than 14MeV. It is important to note that competing reactions have not been accounted for in the experimental calculations. It would not be unreasonable to assume that near the vicinity of the $(n,2n)$ reaction, competing reactions would contribute enough to account for the difference between the theoretical and the experimental values.

TABLE 6.2

 $^{141}\text{Pr}(n,2n)^{140}\text{Pr}$ CROSS SECTION
BY PARALLEL DISK METHOD

Neutron Energy (MeV)	Cross Section (mb)
15.65±.14	1965±161
15.83±.16	2169±174
16.00±.17	2028±162
16.17±.19	2037±163
16.33±.20	1958±155
16.48±.21	1892±149
16.63±.22	2150±167
16.78±.23	1968±152
16.93±.25	2012±155
17.06±.26	1994±154
17.06±.26	1922±148
17.20±.27	1916±146
17.33±.28	1890±144
17.59±.30	1959±149
17.85±.32	2129±162

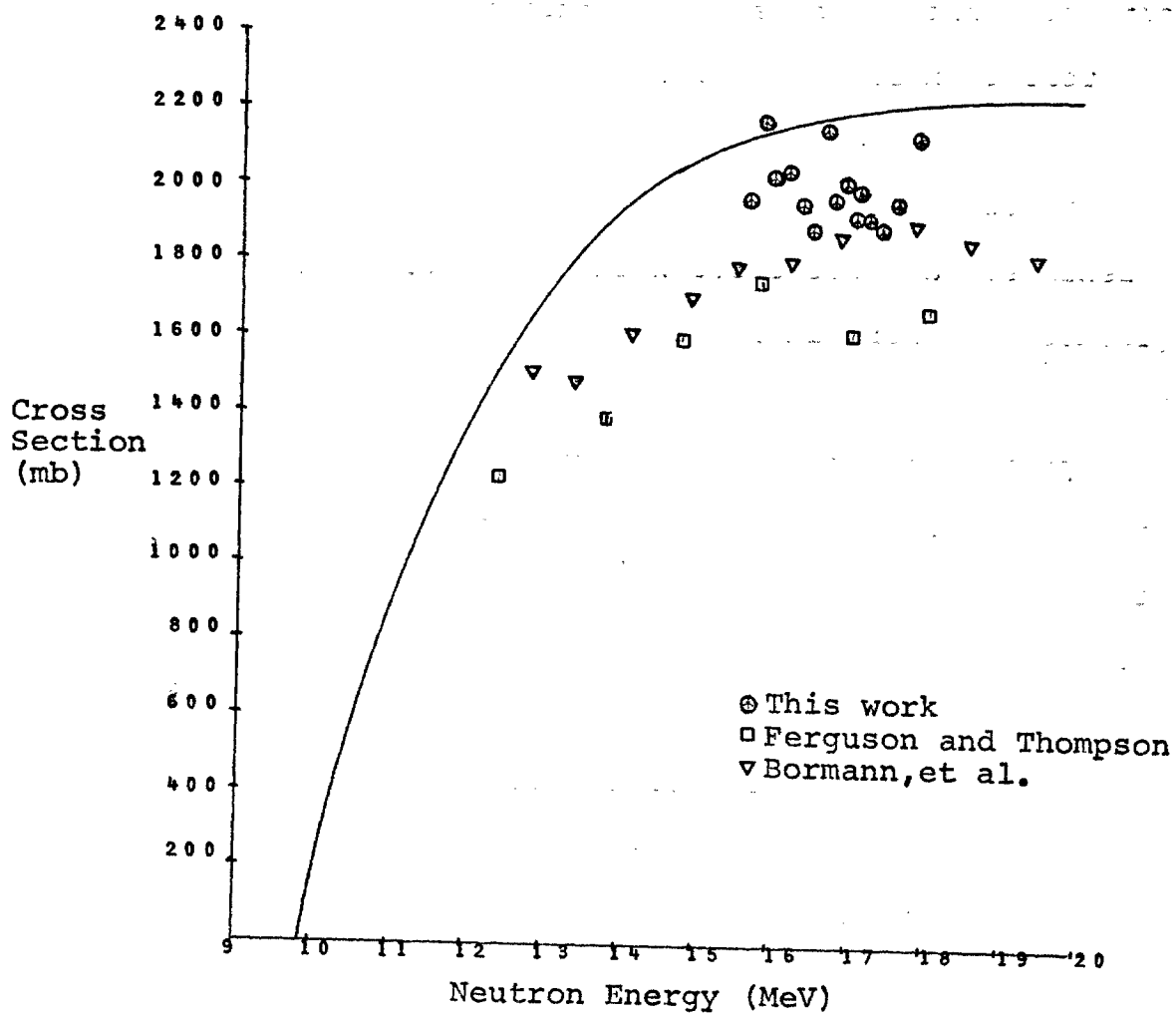


Figure 6.1
Pr Cross Section vs.
Neutron Energy

Two other experiments were attempted as a check on the validity of the parallel disk data; however, insufficient data and target difficulties prevented any conclusions to be made. These experiments, on the other hand, did bring the realization of the importance in a new flux monitor technique.

The powder method²⁶ incorporates the technique by which powdered samples of unknown cross section are mixed with a powdered flux monitor. This eliminated any geometry variations which might be present. The mixture is irradiated and then the resultant activity is followed for several half lives. The absolute activity of each sample at the end of the irradiation period is then determined by least squares analysis, provided the half lives of the samples are well known.

It would have been more desirable to have had a larger range of neutron energies. This can be accomplished by arranging samples behind the tritium target on a circle with center at the end of the target. An apparatus such as a scattering chamber would be useful here, since it would give precise angular readings. Using an experimental method such as this and coupled with the powder method of data reduction, a precise and reliable shape could be given to the excitation function. This is important at a time when fast neutron activation analysis has become useful in trace studies such as air and water pollution.

TABLE I
 $^{63}\text{Cu}(n,2n)^{64}\text{Cu}$ CROSS SECTIONS

Neutron Energy (MeV)	Cross Section (mb)	Reference
12.60±.11	227±14	
12.76±.14	264±17	
12.98±.17	315±21	
13.10±.18	340±22	
13.54±.22	450±30	
13.70±.23	479±32	
14.05±.25	554±38	
14.24±.26	575±39	
14.42±.26	598±41	
14.80±.27	619±42	
14.99±.27	660±44	23
15.18±.26	715±48	
15.55±.24	738±49	
15.71±.23	762±50	
16.03±.21	808±53	
16.31±.19	811±51	
16.52±.19	819±51	
16.75±.20	834±49	
16.93±.47	850±57	
17.27±.46	849±56	
17.59±.44	853±56	
17.90±.42	868±56	
18.19±.39	881±57	
18.47±.36	916±59	
18.71±.33	931±59	
18.94±.29	939±59	
19.29±.20	941±58	
19.58±.19	966±57	
13.1	350	
13.3	470	
14.0	445	
14.1	480	
14.5	475	24
15.0	550	
15.2	470	
15.5	530	
15.9	585	
16.1	630	
16.9	540	
17.5	625	
13.2	275	
14.8	640	25
16.8	810	
19.5	950	
12.41±.12	186±19	
12.81±.15	233±21	
13.77±.20	378±34	8
14.74±.27	507±45	
15.78±.32	649±58	
16.96±.34	758±68	
17.98±.34	826±75	

TABLE II

PARAMETERS IN THE EQUATIONS
FOR THE EXPERIMENTAL CROSS SECTION

Parameter	Value	Error	Reference
T(Pr)	3.38 min	.01 min	2
T(Cu)	9.9 min	.01 min	2
B(Pr)	.47	.01	1
B(Cu)	.97	.01	1
f(Cu)/f(Pr)	1.0	0.0	12
G(Cu)/G(Pr)	1.0	0.0	12
P(Pr)	1.0	0.0	1
P(Cu)	.69	0.0	1

TABLE III

CAMERON'S* PARAMETERS USED IN THE EQUATIONS
FOR THE THEORETICAL CROSS SECTION

Parameter	Value (MeV ⁻¹)
a ₀ (Z)	3.54270
a ₁ (Z)	2.91280
a ₂ (Z)	2.95300
a ₃ (Z)	2.68350
a ₄ (Z)	2.05714
a ₀ (N)	.79360
a ₁ (N)	2.24950
a ₂ (N)	-3.12110
a ₃ (N)	5.85450
a ₄ (N)	3.67937

*Reference 19

Appendix B

MARSHEN

THIS PROGRAM CALCULATES THE MEAN NEUTRON BOMBARDING ENERGY OF NEUTRONS STRIKING A SAMPLE, PRODUCED FROM THE $3T(D,N)4HE$ REACTION, AND ALSO THE REACTION CROSS SECTION FOR A SAMPLE RELATIVE TO A WELL KNOWN MONITOR CROSS SECTION.

DEFINITIONS

ITYPE=METHOD OF CALCULATION, PARALLEL DISK=1, POWDER=2
XNPS=ACTIVITY OF SAMPLE
XNPM=ACTIVITY OF MONITOR
AS=ATOMIC NUMBER OF SAMPLE
AM=ATOMIC NUMBER OF MONITOR

ALPHS=INTERNAL CONVERSION COEFFICIENT FOR SAMPLE
ALPHM=INTERNAL CONVERSION COEFFICIENT FOR MONITOR

TS=HALF LIFE OF SAMPLE
TM=HALF LIFE OF MONITOR

BS=BRANCHING RATIO TO THAT PARTICULAR ENERGY LEVEL FOR SAMPLE
BM=BRANCHING RATIO TO THAT PARTICULAR ENERGY LEVEL FOR MONITOR

FS=EFFICIENCY OF DETECTOR AT THAT PARTICULAR ENERGY FOR SAMPLE
FM=EFFICIENCY OF DETECTOR AT THAT PARTICULAR ENERGY FOR MONITOR

GS=FRACTION OF GAMMAS INTERCEPTED BY DETECTOR FOR SAMPLE
GM=FRACTION OF GAMMAS INTERCEPTED BY DETECTOR FOR MONITOR

XMS=MASS OF THE SAMPLE
XMM=MASS OF THE MONITOR

TI=IRRADIATION TIME

TS1=TIME FROM BEAM OFF TO START OF COUNTING FOR SAMPLE
TS2=TIME FROM BEAM OFF TO STOP OF COUNTING FOR SAMPLE
TM1=TIME FROM BEAM OFF TO START OF COUNTING FOR MONITOR
TM2=TIME FROM BEAM OFF TO STOP OF COUNTING FOR MONITOR

PS=PERCENTAGE ABUNDANCE OF THAT PARTICULAR ISOTOPE FOR SAMPLE
PM=PERCENTAGE ABUNDANCE OF THAT PARTICULAR ISOTOPE FOR MONITOR

SIGMAM=MONITOR CROSS SECTION AT THAT NEUTRON ENERGY
SIGMAS=CALCULATED CROSS SECTION FOR SAMPLE AT THAT PARTICULAR
NEUTRON BOMBARDING ENERGY

DT=UNCERTAINTY IN THE TIMES TS1,TS2,TM1,TM2 (ALL PRESUMED EQUAL)
 DTI=UNCERTAINTY IN THE BOMBARDING TIME, TI
 DX=UNCERTAINTY IN THAT QUANTITY X, WHEREX=ALPHS,ALPHM,FS,FM,GS,
 GM,XMS,XMM,PS,PM,TS,TM,OR SIGMAM

RT=RADIUS OF TRITIUM TARGET
 DR=INCREMENT OF TARGET RADIUS
 S=RADIUS OF SAMPLE
 D=DISTANCE BETWEEN TARGET AND SAMPLE
 DTT=INCREMENT OF ANGLE
 XMA=REST MASS ENERGY OF ALPHA PARTICLE
 XMD=REST MASS ENERGY OF DEUTRON
 XMN=REST MASS ENERGY OF NEUTRON
 Q=Q-VALUE FOR THE $3T(D,N)4HE$ REACTION
 ED=KINETIC ENERGY OF DEUTERON IN LAB SYSTEM (MEV)
 EN=KINETIC ENERGY OF NEUTRON IN LAB SYSTEM (MEV)

IMPLICIT REAL *8(A-H,O-Z)
 DIMENSION THETA(180),XR(300)
 DATA XMA,XMN, XMD,Q/3726.98DO,939.505DO,1875.49DO,
 * 17.577DO/
 SIN(U)=DSIN(U)
 COS(G)=DCOS(G)
 TAN(U)=DTAN(U)
 ATAN(P)=DATAN(P)
 SORT(U)=DSQRT(U)
 ABS(X)=DABS(X)
 EXP(X)=DEXP(X)

WRITE(6,2)
 WRITE(6,3)

1 FORMAT(16X,F7.4,3H+/-,F6.4,10X,F7.2,3H+/-,F6.2)
 2 FORMAT(16X,7HNEUTRON,3X,5HERROR,11X,5HCROSS,5X,
 * 5HERROR)
 3 FORMAT(16X,6HENERGY,20X,7HSECTION,/
 4 FORMAT(11)
 5 FORMAT(5E10.4)
 6 FORMAT(6E10.4)
 7 FORMAT(7E10.4)
 READ(5,4) ITYPE
 READ(5,5) RT,DR,S,D,DTT
 READ(5,7) AS,ALPHS,TS,BS,FS,GS,PS
 READ(5,7) AM,ALPHM,TM,BM,FM,GM,PM
 READ(5,7) DALPHS,DTS,DBS,DES,DGS,DPS,DT
 READ(5,6) DALPHM,DTM,DBM,DEM,DGM,DPM
 14 READ(5,7,END=69) ED,SIGMAM,DSIGM,XMS,DXMS,XMM,DXMM
 READ(5,7) XNPS,XNPM,T1,TS1,TS2,TM1,TM2
 XLS=.69315/TS
 XLM=.69315/TM
 EXS=EXP(-XLS*TI)
 EXM=EXP(-XLM*TI)
 I=(ITYPE-1)99,99,100

CALCULATION OF CROSS SECTION FOR PARALLEL DISK METHOD

```

99 EXS1=EXP(-XLS*TS1)
   EXS2=EXP(-XLS*TS2)
   EXM1=EXP(-XLM*TM1)
   EXM2=EXP(-XLM*TM2)
   GOD=(1.+ALPHS)*XNPS*AS*TM/((1.+ALPHM)*XNPM*AM*TS)
   DAMN=BM*FM*GM*XMM*PM*SIGMAM/(BS*FS*GS*XMS*PS)
   THE=(1.-EXM)*(EXM1-EXM2)
   WAR=1./((1.-EXS)*(EXS1-EXS2))
   SIGMAS=GOD*DAMN*THE*WAR
   VAR=1./XNPS+1./XNPM+(DBS/BS)**2+(DBM/BM)**2
   VAR=VAR+(DFS/FS)**2+(DFM/FM)**2+(DGS/GS)**2
   VAR=VAR+(DGM/GM)**2+(DXMS/XMS)**2+(DXMM/XMM)**2
   VAR=VAR+(DALPHS/(1.-ALPHS))**2+(DALPHM/(1.-ALPHM))**2
   VAR=VAR+(DPS/PS)**2+(DPM/PM)**2
   VAR=VAR+((XLS*EXS1*DT)/(EXS1-EXS2))**2
   VAR=VAR+((XLS*EXS2*DT)/(EXS1-EXS2))**2
   VAR=VAR+((XLM*EXM1*DT)/(EXM1-EXM2))**2
   VAR=VAR+((XLM*EXM2*DT)/(EXM1-EXM2))**2
   VAR=VAR+(((XLM*EXM)/(1.-EXM)
*      -(XLS*EXS)/(1.-EXS))*DT/TI)**2
   VAR=VAR+((1.+XLM*(TM1*EXM1-TM2*EXM2
*      -TI*EXM))*DTM/TM)**2
   VARA=(TS1*EXS1-TS2*EXS2)/(EXS1-EXS2)
   VAR=VAR+((1.+XLS*(VARA-TI*EXS/(1.-EXS)))*DTS/TS)**2
   VAR=SQRT((VAR+(DSIGM/SIGMAM)**2)*SIGMAS*SIGMAS)
   GO TO 101

```

CROSS SECTION BY POWDER METHOD

```

100 GOD=(1.+ALPHS)*XNPS*AS/((1.+ALPHM)*XNPM*AM)
    BLESS=BM*FM*GM*XMM*PM*SIGMAM/(BS*FS*GS*XMS*PS)
    PEACE=(1.-EXM)/(1.-EXS)
    SIGMAS=GOD*BLESS*PEACE
    VAR=1./XNPS+1./XNPM+(DBS/BS)**2+(DBM/BM)**2
    VAR=VAR+(DFS/FS)**2+(DFM/FM)**2+(DGS/GS)**2
    VAR=VAR+(DGM/GM)**2+(DXMS/XMS)**2+(DXMM/XMM)**2
    VAR=VAR+(DALPHS/(1.-ALPHS))**2+(DALPHM/(1.-ALPHM))**2
    VAR=VAR+(DPS/PS)**2+(DPM/PM)**2
    VAR=VAR+((TI*EXS/(1.-EXS))*DTS/TS)**2
    VAR=VAR+((TI*EXM/(1.-EXM))*DTM/TM)**2
    VAR=SQRT((VAR+(DSIGM/SIGMAM)**2)*SIGMAS*SIGMAS)
    GO TO 101

```

CALCULATION OF NEUTRON BOMBARDING ENERGY

```

101 K=RT/DR
    STUD=0.0
    SUMA=0.0
    SUMEA=0.0
    ED=ED/1000.

```



```

B ( (XMA-XMD) *ED+XMA*Q) / (XMA+XMN)
IMAX=ATAN ( (RT+S)/D) *180./ (3.14159*DTT)
DO 25 I=1,IMAX
XX=0.0
THETA (I)=3.14159*DTT*I/180.
A=SQRT (XMN*XMD*ED) *COS (THETA (I)) / (XMA+XMN)
ROOT=A+SQRT (A*A+B)
EN=ROOT*ROOT
RPRIME=D*SQRT (1.+TAN (THETA (I)) *TAN (THETA (I)))
V=D*TAN (THETA (I))
W=V*COS (THETA (I))
DO 24 J=1,K
XR (J)=DR*J
Y=(S*S+XR (J) *XR (J) -V*V) / (2.*XR (J))
X=SQRT (ABS (V*V- (Y-XR (J)) **2 ))
IF (V-S) 15,15,17
15 IF (XR (J)+V-S) 18,18,16
16 IF (XR (J)-Y) 19,19,20
17 IF (XP (J)+S-V) 21,21,20
18 PHIMAX=2.*3.14159
GO TO 22
19 PHIMAX=3.14159/2.+ATAN (ABS (X/(Y-XR (J))))
GO TO 22
20 PHIMAX=ATAN (ABS (X/(Y-XR (J))))
GO TO 22
21 DA=0.0
GO TO 23
22 DA=2.*RPRIME*W*PHIMAX
23 AREA=DA*DTT/3.14159
XX=XX+AREA/100.
24 CONTINUE
SUMEA=EN*XX+SUMEA
SUMA=XX*SUMA
EMEAN=SUMEA/SUMA
STUD=XX*EN*EN+STUD
STDEV=SQRT (ABS (SUMA*STUD-SUMEA*SUMEA)) /SUMA
ANGLE=THETA (I) *180./3.14159
25 CONTINUE
WRITE (6,1) EMEAN,STDEV,SIGMAS,VAR
GO TO 14
69 CALL EXIT
END

```

REFERENCES

1. C. M. Lederer, et al., "Table of Isotopes" (John Wiley and Sons, Inc., New York, 1967), 6th ed.
2. Thomas G. Ebrey and P. R. Gray, Nuclear Physics, Vol. 61, 479 (1965)
3. L. A. Rayburn, Physical Review, Vol. 122, 168 (1961)
4. E. B. Paul and R. L. Clarke, Canadian Journal of Physics, Vol. 31, 267 (1953)
5. P. Cuzzocrea, et al., Nuovo Cimento, Vol. 52, 476 (1967)
6. C. S. Khurana and H. S. Hans, Nuclear Physics, Vol. 28, 560 (1961)
7. R. G. Wille and R. W. Fink, Physical Review, Vol. 118, 242 (1960)
8. J. M. Ferguson and W. E. Thompson, Physical Review, Vol. 118, 228 (1960)
9. M. Bormann, A. Behrend, I. Riehle, O. Vogel, Nuclear Physics, A115, 309 (1968)
10. V. F. Weisskopf and D. H. Ewing, Physical Review, Vol. 57, 452 (1940)
11. F. E. Verling, et al., "A Consistent Set of Q-Values", Nuclear Data Tables, Part 2, U.S. Government Printing Office (1960)
12. Richard Lear, Masters Thesis, NTSU (1969)
13. George Pepper, Masters Thesis, NTSU (1969)
14. M. B. Stout, Basic Electrical Measurements (Prentice-Hall, Inc., Englewood Cliffs, N. J., 1965), p.45
15. J. M. Blatt and V. F. Weisskopf, Theoretical Nuclear Physics (John Wiley and Sons, Inc., New York, 1952)
16. Niels Bohr, Science, Vol. 86, 161 (1937)
17. R. G. Moore, Jr., Reviews of Modern Physics, Vol. 32, 101 (1960)

18. V. F. Weisskopf, *Physical Review*, Vol. 52, 295 (1937)
19. A. G. W. Cameron, *Canadian Journal of Physics*, Vol. 36, 1040 (1958)
20. Ronald White, Unpublished Masters Thesis (1970)
21. S. J. Bame, Jr. and J. E. Perry, Jr., *Physical Review*, Vol. 107, 1616 (1957)
22. A. Paulsen and H. Liskien, *Nuclear Physics*, Vol. 56, 394 (1964)
23. H. Liskien and A. Paulsen, *Journal of Nuclear Energy*, Vol. 19, 73 (1964)
24. A. V. Cohen and P. H. White, *Nuclear Physics*, Vol. 1, 73 (1956)
25. J. E. Brolley, Jr., J. L. Fowler, and L. K. Schlacks, *Physical Review*, Vol. 88, 618 (1952)
26. P. V. Rao and R. W. Fink, *Physical Review*, Vol. 154, 1023 (1967)